Spectral analysis of photo-induced delayed luminescence from mesenchymal stem cells for label-free cell viability assessment*

BAI Hua (白华)[1], **LIU Jie** (刘杰)[1], **CHEN Wei** (陈微)[2], **SHI Jia** (石嘉)[1]**, **CHEN Hongli** (陈洪丽)[1,2], **YAN Shulin** (严淑琳)[3,4], **ZHANG Jianzhong** (张建中)[3,4], and **HAN Zhibo** (韩之波)[3,4,5]

1. *Tianjin Key Laboratory of Optoelectronic Detection Technology and Systems, School of Electronic and Information Engineering, Tiangong University, Tianjin 300387, China*
2. *College of Life Science, Tiangong University, Tianjin 300387, China*
3. *Tianjin Key Laboratory of Engineering Technologies for Cell Phamaceutical, Tianjin 300457, China*
4. *National Engineering Research Center of Cell Products / AmCellGene Co., Ltd., Tianjin 300457, China*
5. *State Key Lab of Experimental Hematology, Chinese Academy of Medical Sciences & Peking Union Medical College, Tianjin 300020, China*

(Received 14 November 2020; Revised 29 December 2020)

In this work, the spectral properties of the photo-induced delayed luminescence (DL) from mesenchymal stem cells (MSCs) and their correlation with cell viability were investigated using the single photon counting combined with band-pass filters. The results show that the DL of MSCs has a broad spectral distribution, which covers from 300 nm to 650 nm at least. The DL spectrum is not evenly distributed, but mainly distributed in the range from 400 nm to 550 nm. In addition, the DL spectral distribution remains stable during the DL decay process. Compared with the DL spectra of MSCs with high viability (>80%), those of MSCs with low viability (<30%) show a significant red-shift, referring to the increase in the proportion of 572—650 nm band and the decrease in the proportions of both 315—436 nm band and 413—500 nm band. Furthermore, the degree of the DL spectral red-shift exhibits a monotonous change as MSCs' viability decreases, and thus can be used as an important indicator for the cell viability assessment.

Document code: A **Article ID:** 1673-1905(2021)06-0373-6

DOI https://doi.org/10.1007/s11801-021-0181-8

Mesenchymal stem cells (MSCs) are a type of pluripotent stem cells derived from mesoderm and ectoderm[1]. MSCs have a strong proliferative capacity[2], immunoregulatory function[3], and the ability to differentiate into osteoblasts, chondrocytes, adipocytes, muscle cells, etc[4]. These advantages make MSCs have great clinical application potential and industrial development prospects in the treatment of autoimmune diseases and regenerative medicine.

Obviously, cell viability is a key factor affecting the in vitro culture and clinical application of MSCs. Nowadays, cell viability is mainly detected by biochemical methods such as MTT[5], XTT[6] and trypan blue[7]. However, most of these methods such as labeling and staining are invasive, which will change the cell's living environment and even cause irreversible cell damage or death, and thus make the tested cells cannot be further cultured or applied. Therefore, it is necessary to develop label-free and non-invasive cell viability detection.

Over the past few decades, the photo-induced delayed luminescence (DL), a natural phenomenon that is ubiquitous in living organisms, has attracted widespread attention and is expected to obtain information on the functions and physiological status of biological systems. Since the first discovery of DL from plants in the 1950s[8], a number of experiments have shown that the DL properties are closely related to the bio-systems' characteristics such as biological activity[9], injury[10], physiological and pathological changes[11], etc., as well as the surrounding environment[12]. Therefore, DL has the potential to reflect the biological effects caused by internal changes in organisms and external environmental factors, and to provide comprehensive indicators that reflect the intrinsic characteristics of bio-systems.

* This work has been supported by the National Natural Science Foundation of China (Nos.61201106, 61905177 and 61705164), the Tianjin Research Program of Application Foundation and Advanced Technology (Nos.14JCQNJC01800, 19JCQNJC01400 and 19JCQNJC01600), and the Tianjin Special Program of Science and Technology (Nos.19JCTPJC47900 and 2018KJ214).
** E-mail: shijia@tiangong.edu.cn

Due to the sensitive bio-sensing performance, DL is increasingly applied in many fields, such as seed quality assessment[13], detection of environmental pollution[14], and identification of Chinese herbal medicines[15]. In recent years, encouraging progress has also been made in the study of DL from cultured mammalian cells. For example, F. Musumeci et al found that human fibroblasts and human melanoma cells have significant differences in DL spectral distribution, and demonstrated that DL has the potential to be a powerful non-invasive tool for skin cancer detection[16]. I. Baran et al studied the effects of the treatments with quercetin, menadione, H_2O_2 and their combinations on the DL from Human Leukemia Jurkat T-cells, and proposed that the Complex I of the mitochondrial respiratory chain may be an important source of DL from Jurkat T-cells[17]. A. Scordino et al found a correlation between DL from thyroid tumor cells and their induced apoptosis by berberine, and suggested that the decrease of the DL blue component may be a hallmark of the induced apoptosis[18]. Rosaria Grasso et al found that ferulic acid and nano lipid carrier had synergistic pro-apoptotic effect on glioblastoma cells, and the mechanism was reasonably explained based on DL spectra[19]. In our previous studies, we found the significant differences in the DL decay kinetics between MSCs with high and low viabilities[20]. These findings strongly prove that DL has a great potential to reflect changes in cell physiology and pathology sensitively.

In this paper, we focus on the spectral properties of DL from MSCs and their correlation with cell viability. This work may be helpful to develop a new label-free and non-invasive cell viability detection method, and also provide new evidences for exploring the mechanisms of DL from cells.

We isolated MSCs from human Umbilical Cord (hUC) tissues by the method previously described[21]. Briefly, the hUC was minced and digested. Cells were plated at a density of 10 000 cells/cm^2 to 16 000 cells/cm^2 in a T75 cell culture flask (Corning, USA) in D-MEM/F-12 (Gibco, USA) culture medium supplemented with 10% fetal bovine serum (FBS) (Hyclone, USA) and 10 ng/mL epidermal growth factor (Sigma, USA) at 37 ℃ under 5% CO_2. After the cells covered 90% of the bottom of the cell culture flask, the cells were digested with trypsin (Gibco, USA) to remove the residual culture solution, and PBS was added to prepare cell suspension for experiments.

The cell viability was assessed using the trypan blue method. The cells were suspended in PBS with a cell concentration of 1×10^5/mL. 20 μL cell suspension was then mixed with 20 μL 0.4% trypan blue solution (Sigma, USA). The mixture was dropped into a blood count plate and observed by a microscope (Olympus, Japan). The numbers of viable and dead cells were counted respectively, and the cell viability is defined as the ratio of the number of viable cells to the total number of all cells.

The experiments were carried out on the biophoton detection system established by ourselves, as shown in Fig.1. A xenon lamp (Zolix, China) was adopted as the excitation source, and the power of the excitation light irradiating the sample was 6.2 mW. Two silica fibers were used to transmit excitation light and signal light, respectively. DL signal from the sample was detected by a photon counting head device (H7360-01, HAMAMATSU, Japan), containing a 25-mm head-on PMT, high-voltage power supply circuit and photon counting circuit. The dark count of the detector is 18 /s, and the spectral response of the detector is from 300 nm to 650 nm. The electrical pulses output by the detector were counted by a gated photon counter (PMS-400A, Becker & Hickl, Germany) with two fast gated photon-counting and multiscaler channels. Two shutters were used to ensure that DL was detected after shutting off irradiation. A timing controller was used to output electrical signals, which control the two shutters and the photon counter to operate in coordination.

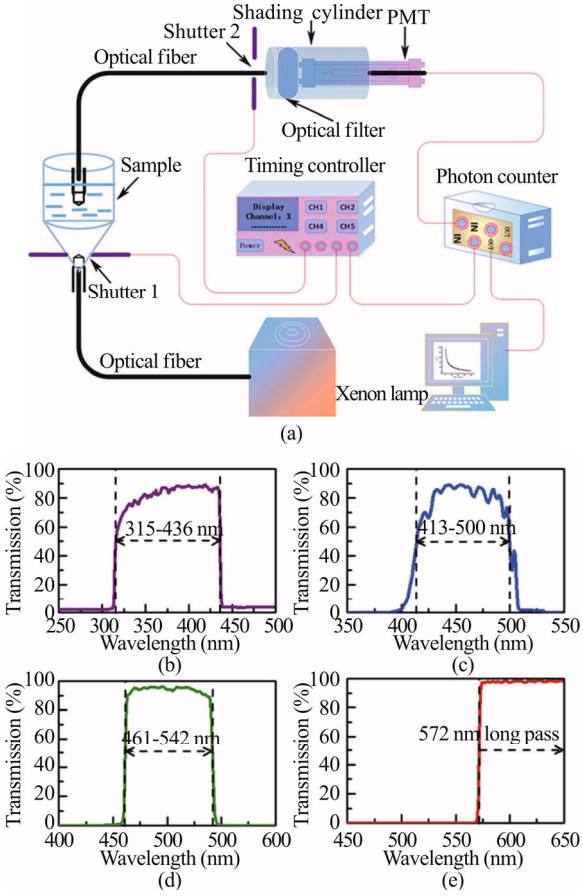

Fig.1 (a) Schematic diagram of the biophoton detection system; (b) Transmission spectrum of 315—436 nm; (c) Transmission spectrum of 413—500 nm; (d) Transmission spectrum of 461—542 nm; (e) Transmission spectrum of 572—650 nm

To measure the different spectral components of DL, four filters were used, whose transmission wavelength

ranges are 315—436 nm, 413—500 nm, 461—542 nm, and 572 nm long pass respectively, as shown in Fig.1. In particular, since the spectral response of the PMT is 300—650 nm, the use of the 572 nm long-pass filter results in a transmission wavelength range of 572—650 nm. The main features including the bandwidth, average transmittance and average count sensitivity of the four bands are listed in Tab.1.

Tab.1 Main features of the bands

Band	Bandwidth	Average transmittance	Average count sensitivity
315—436 nm	121 nm	81.7%	2.1×10^5 /s/pW
413—500 nm	87 nm	79.5%	2.2×10^5 /s/pW
461—542 nm	81 nm	92.9%	1.7×10^5 /s/pW
572—650 nm	78 nm	97.5%	0.36×10^5 /s/pW

For DL measurement, MSCs were suspended in PBS at a concentration of 2×10^7 /mL, and the 0.2 mL cell suspension was dropped into the sample pool. In each DL acquisition, the irradiation duration was 1 s, and the DL started to be recorded 40 ms after stopping irradiation. The DL was recorded for 2 s with the unit signal collection duration of 10 ms. Due to the ultra-weak intensity of DL, 50 repeated acquisitions were accumulated for a measurement. The phototoxicity of MSCs was tested by the Trypan Blue method, and the viability of the measured cells was not significantly different from that of the control.

A typical spectral distribution of DL from MSCs with high viability is shown in Fig.2. It can be seen from Fig.2(a) that the intensities of the different bands show great differences. Among them, the 413—500 nm band has the highest intensity, Next is the 461—542 nm band, whose intensity is about 70% of the former. In contrast, the bands corresponding to 315–436 nm and 572—650 nm have a much smaller contribution to the DL. In order to display the DL spectral distribution visually, we normalize the single spectral intensities to the value of their sum and show them in Fig.2(b). Considering that the measurement results are directly affected by the experimental set-up parameters listed in Tab.1, we correct the photon count of each band using the following algorithm.

$$Relative\ intensity = \frac{Photon\ count}{BT \times T \times S}, \tag{1}$$

where BW and T represent the bandwidth and the average transmittance respectively of a filter, and S represents the average photon counting sensitivity of the PMT corresponding to the transmission band. The corrected DL spectrum is shown in the light blue histogram in Fig.2(b). Compared with the spectrum before correction, the proportions of 315—436 nm and 413—500 nm bands in the corrected spectrum decrease, while those of 461—542 nm and 572—650 nm bands increase. However, the two have no significant changes in the shape of the spectral distribution. It can be seen that the DL from MSCs has a broad spectral distribution, covering at least 300—650 nm. In addition, the spectral distribution is not evenly, but mainly concentrated in 400—550 nm.

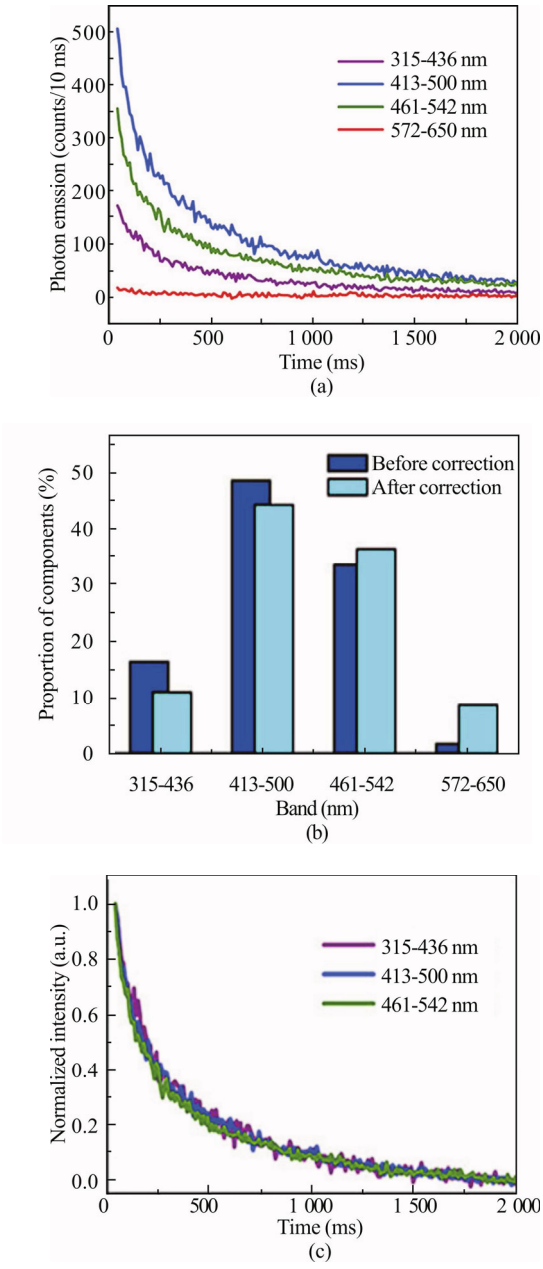

Fig.2 (a) Typical DL emission spectra of MSCs dynamics of different spectral components of DL from MSCs; (b) Spectra obtained by normalizing the single spectral intensities to the value of their sum before correction (blue bars) and after correction (bright blue bars); (c) Comparison of normalized DL dynamics in different bands

In order to observe the differences in the DL dynamics of these bands, we normalize the DL curves of the 315—436 nm, 413—500 nm and 461—542 nm bands using the Min-Max Normalization, as shown in Fig.2(c). It should be mentioned that due to the low sensitivity of

the PMT in the 572—650 nm band, the measured DL is too weak to show accurate dynamic characteristics, so this band is not normalized for comparison. It can be seen that the 315—436 nm, 413—500 nm, and 461—542 nm bands have the same dynamic characteristics, indicated by the high coincidence of the normalized DL curves. The results indicate that although the DL intensity of MSCs decays with time, the spectral distribution remains stable during the DL process.

In order to study whether the DL spectral distribution is related to cell viability, we first focus on the differences in DL spectra between high and low viability. In our experiment, the decrease of the cell viability was induced by the starvation method, which is to suspend the cells in PBS at a low temperature of 4 °C for several days[22]. We used the cells with viability >80% (by trypan blue method) as high-viability cells and those with viability <30% as low-viability cells to highlight the differences in cell viability. The comparison of DL spectral distribution between high and low viability is shown in Fig.3. It can be seen that compared to the DL spectra of cells with high viability, the proportions of 315—436 nm and 413—500 nm bands of those with low viability decrease by about 34% and 27% respectively, the proportion of 572—650 nm band increases by about 2 times, while the proportion of 461—542 nm band has no obvious change. Further, the Student's t-test was used for statistical analysis. The results show that the differences in the 315—436 nm, 413—500 nm and 572—650 nm bands are significant, as indicated by the p values of 9.37×10^{-5}, 1.49×10^{-6} and 8.51×10^{-6} respectively, while the 461—542 nm does not show significant difference, as indicated by the p values of 0.808. These results reveal an obvious spectral red-shift that appears in the DL spectra of low-viability MSCs. This red-shift may be a valuable indicator of the cell viability decline.

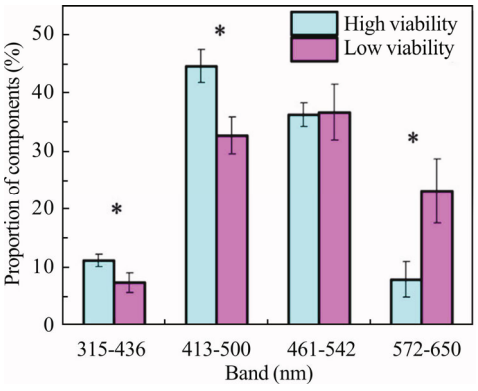

Fig.3 Comparison of DL spectral distributions between high and low viability of MSCs (All data are corrected according to Eq.(1); * indicates p<0.05.)

Considering that only the differences between high and low viability are not enough to prove the effectiveness of DL spectral distribution as an indicator, we further studied the change of DL spectral distribution with the decrease of cell viability. Here, the decrease of cell viability was induced by placing the cells under a condition of starvation, as mentioned above. The cell viability was accessed using the trypan blue method in parallel with the DL spectral measurements every 6 h during the decline of cell viability. As shown in Fig.4, the cell viability undergoes a monotonous decline with time of cell starvation. Correspondingly, the proportions of $I_{315–436}$ and $I_{413–500}$ show a downward trend, while the proportion of $I_{572–650}$ exhibits a significant increase. The results indicate that the entire process of cell viability decline is accompanied by the DL spectral red-shift, and the degree of red-shift is related closely to the cell viability. However, it is noticed that anyone of the $I_{315–436}$, $I_{413–500}$ and $I_{572–650}$ does not exhibit good monotonicity as the cell viability decreases, and thus cannot be used as an indicator. Therefore, we define a comprehensive indicator as follows

$$RS = \frac{I_{315–436} + I_{413–500}}{I_{572–650}}. \tag{2}$$

Obviously, RS can reflect the degree of DL spectral red-shift more sensitively and accurately than anyone of the $I_{315–436}$, $I_{413–500}$ and $I_{572–650}$. The smaller the RS, the higher the degree of the spectral red-shift. As a result, compared with the cases of $I_{315–436}$, $I_{413–500}$ and $I_{572–650}$, the change of RS with cell-starvation time presents much better monotonicity and smaller standard deviations, indicating that RS is more sensitive to the changes of the cell viability, and less affected by individual differences of the cells. Based on these findings, we suggest that RS can be an effective spectral marker for assessment of MSC viability.

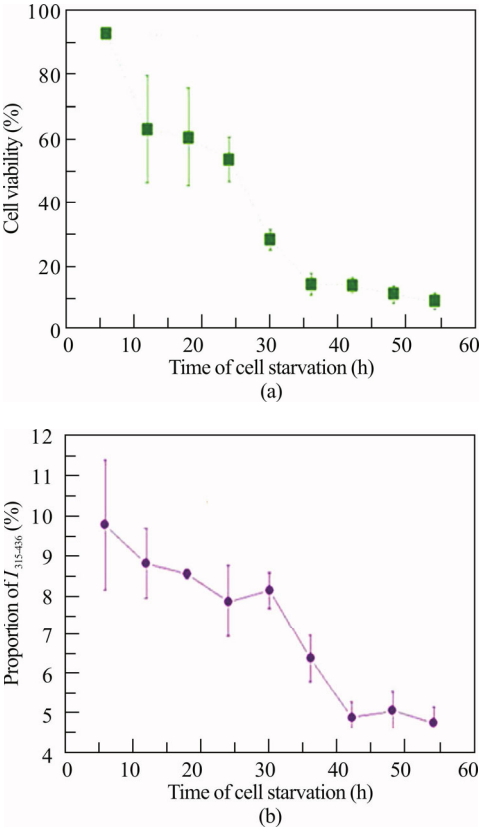

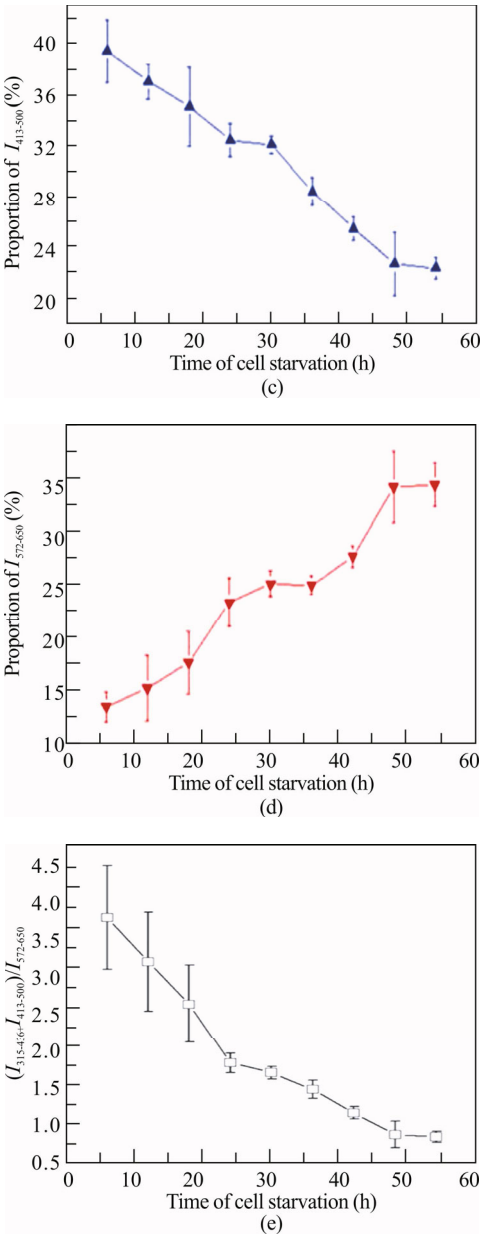

Fig.4 Changes of cell viability and DL spectral distribution with time of cell starvation: (a) Cell viability accessed by the trypan blue method; Changes in the proportions of (b) $I_{315–436}$, (c) $I_{413–500}$ and (d) $I_{572–650}$ with time of cell starvation; (e) Change of the radio of ($I_{315–436}$+$I_{413–500}$) to $I_{572–650}$ with time of cell starvation

DL is a re-luminescence process of organisms after illumination. It is generally considered that this process is different from phosphorescence and delayed fluorescence, whose luminescence lifetimes are generally on the order of microseconds[23,24]. In our study, the DL of MSCs was collected 40 ms after the illumination was stopped, which is beneficial to reduce the interference of phosphorescence and delayed fluorescence. Essentially, photon emission originates from the radiation transition of excited molecules from high-level electronic states to low-level electronic states, and its wavelength depends on the energy level structure of the molecules. The results in Fig.2 show that the DL spectrum of the cell covers at least the ultraviolet and visible wavelengths (300—650 nm). This broad spectral distribution suggests that the DL of MSCs is not derived from a specific biomolecule, but a variety of biomolecules are involved. It is worth noting that the DLs of different bands exhibit the same decay characteristics, although their intensities are different, as shown in Figs.2(a) and (c). This result indicates that the DL components derived from multiple biomolecules in the cells may have the same source. Considering these results comprehensively, we believe that the DL may originate from the coherent photon field in the cells[25]. Since the cells contain a large amount of endogenous fluorescent substances, such as aromatic amino acids, NADH, flavin, lipopigments, etc[26,27], only a small part of the photons that escape from the coherent photon field may be directly collected by the detector, while the rest of the photons may induce the fluorescence of these biomolecules, resulting in a broad DL spectral distribution.

Fig.3 shows a significant red shift in the DL spectrum of low-viability cells relative to high-viability cells. This may be caused by changes in the composition of endogenous fluorescent molecules in cells. And these results are similar to those of Agata Scordino et al[18] which showed that the DL blue component (about 420—500 nm) of the apoptotic thyroid cancer cells induced by berberine exhibited a strong decrease, and this decrease could be linked to the NADH oxidation and an irreversible decrease of intramitochondrial NADH pool[28]. Therefore, we infer that as the viability of MSCs decreases, the reduction of NADH may be the main cause for the decrease in the proportion of the 413—500 nm band, while the increase in the proportion of 572—650 nm band may be related to the lipopigments, whose fluorescence emission wavelength is about 570 nm[16,26].

Further, we found that the DL spectral red-shift continued to occur during the decline of the cell viability, as shown in Fig.4. It is worth noting that with the decrease of the cell viability, the degree of DL spectral red-shift is not linearly related to the result by the trypan blue method. Although this can be partly attributed to measurement errors, it also suggests that the DL may reflect more biological information than the trypan blue method. Compared with the trypan blue method that can only distinguish between living and dead cells, DL may not only reflect the cell viability, but also be sensitive to the changes in the vitality of living cells, which provides a new guidance for our future research.

In this study, it was found that the DL from MSCs has a stable spectral distribution during its decay process, which covers at least 300—650 nm, and mainly distributes in 400—550 nm. Further, we demonstrated that the decrease in the cell viability is accompanied by the DL spectral red-shift, which can be represented by an increase in the proportion of 572—650 nm band and a decrease in the proportions of both 315—436 nm band and

413—500 nm band. The degree of this red-shift has the potential to act as an important spectral signature for label-free assessment of the cell viability.

References

[1] D. J. Prockop, Science **276**, 71 (1997).

[2] W. Wagner, F. Wein, A. Seckinger, M. Frankhauser, U. Wirkner, U. Krause, J. Blake, C. Schwager, V. Eckstein, W. Ansorge and A. D. Ho, Exp. Hematol. **33**, 1402 (2005).

[3] X. J. Guan, L. Song, F. F. Han, Z. L. Cui, X. Chen, X. J. Guo and W. G. Xu, J. Cell. Biochem. **114**, 323 (2013).

[4] M. F. Pittenger, M. F. Pittenger, A. M. Mackay, A. M. Mackay, S. C. Beck, S. C. Beck, R. K. Jaiswal, R. K. Jaiswal, R. Douglas, R. Douglas, J. D. Mosca, J. D. Mosca, M. A. Moorman, M. A. Moorman, D. W. Simonetti, D. W. Simonetti, S. Craig, S. Craig, D. R. Marshak and D. R. Marshak, Science **284**, 143 (1999).

[5] D. Gerlier and N. Thomasset, J. Immunol. Methods. **94**, 57 (1986).

[6] D. M. Kuhn, M. Balkis, J. Chandra, P. K. Mukherjee and M. A. Ghannoum, J. Clin. Microbiol. **41**, 506 (2003).

[7] A. K. H. Kwok, C. K. Yeung, T. Y. Y. Lai, K. P. Chan and C. P. Pang, Br. J. Ophthalmol. **88**, 1590 (2004).

[8] B. L. STREHLER and W. ARNOLD, J. Gen. Physiol. **34**, 809 (1951).

[9] E. Costanzo, M. Gulino, L. Lanzanò, F. Musumeci, A. Scordino, S. Tudisco and L. Sui, Eur. Biophys. J. **37**, 235 (2008).

[10] J. Kim, J. Lim, B. C. Lee, Y. U. Kim, K. L. Seung, S. C. Byeung and K. S. Soh, J. Heal. Sci. **51**, 155 (2005).

[11] H. W. Kim, S. B. Sim, C. K. Kim, J. Kim, C. Choi, H. You and K. S. Soh, Cancer Lett. **36**, 823 (2005).

[12] Y. Ikushima, A. Takeuchi, M. Katsumata, Y. Sato and T. Hakamata, J. Lumin. **223**, 117209 (2020).

[13] R. Grasso, M. Gulino, F. Giuffrida, M. Agnello, F. Musumeci and A. Scordino, J. Photochem. Photobiol. B Biol. **187**, 126 (2018).

[14] L. Mielnik and C. Asensio, J. Soils Sediments. **18**, 2844 (2018).

[15] M. Sun, M. He, H. Korthout, M. Halima, H. K. Kim, Y. Yan, E. Van Wijk, R. Van Wijk, C. Guo and M. Wang, Photochem. Photobiol. Sci. **18**, 5 (2019).

[16] F. Musumeci, L. A. Applegate, G. Privitera, A. Scordino, S. Tudisco and H. J. Niggli, J. Photochem. Photobiol. B Biol. **79**, 93 (2005).

[17] I. Baran, C. Ganea, A. Scordino, F. Musumeci, V. Barresi, S. Tudisco, S. Privitera, R. Grasso, D. F. Condorelli, I. Ursu, V. Baran, E. Katona, M. M. Mocanu, M. Gulino, R. Ungureanu, M. Surcel and C. Ursaciuc, Cell Biochem. Biophys. **58**, 169 (2010).

[18] A. Scordino, A. Campisi, R. Grasso, R. Bonfanti, M. Gulino, L. Iauk, R. Parenti and F. Musumeci, J. Biomed. Opt. **19**, 11 (2014).

[19] R. Grasso, P. Dell'Albani, C. Carbone, M. Spatuzza, R. Bonfanti, G. Sposito, G. Puglisi, F. Musumeci, A. Scordino and A. Campisi, Sci. Rep. **10**, 4680 (2020).

[20] P. Chen, X. Li, Y. Wang, H. Bai and L. Lin, Optoelectron. Lett. **10**, 391 (2014).

[21] W. Gong, Z. Han, H. Zhao, Y. Wang, J. Wang, J. Zhong, B. Wang, S. Wang, Y. Wang, L. Sun and Z. Han, Cell Transplant. **21**, 207 (2012).

[22] H. Bai, P. Chen, H. Fang, L. Lin, G. Q. Tang, G. G. Mu, W. Gong, Z. P. Liu, H. Wu, H. Zhao and Z. C. Han, Laser Phys. Lett. **8**, 78 (2011).

[23] S. Chao, M. R. Holl, S. C. McQuaide, T. T. H. Ren, S. A. Gales and D. R. Meldrum, Opt. Express **15**, 10681 (2007).

[24] J. Partee, E. L. Frankevich, B. Uhlhorn, J. Shinar, Y. Ding and T. J. Barton, Phys. Rev. Lett. **82**, 3673 (1999).

[25] F. A. Popp, K. H. Li, W. P. Mei, M. Galle and R. Neurohr, Experientia **44**, 576 (1988).

[26] A. C. Croce, A. Spano, D. Locatelli, S. Barni, L. Sciola and G. Bottiroli, Photochem. Photobiol. **69**, 364 (1999).

[27] H. Andersson, T. Baechi, M. Hoechl and C. Richter, J. Microsc. **191**, 1 (1998).

[28] I. Baran, C. Ganea, S. Privitera, A. Scordino, V. Barresi, F. Musumeci, M. M. Mocanu, D. F. Condorelli, I. Ursu, R. Grasso, M. Gulino, A. Garaiman, N. Musso, G. A. P. Cirrone and G. Cuttone, Oxid. Med. Cell. Longev. **2012**, 498914 (2012).